MULTISCALE OBSERVATION AND MODELING OF CRACK INITIATION IN WOVEN COMPOSITES

Martin Hirsekorn[1], Aurélien Doitrand[1], Robin Naylor[1] and Christian Fagiano[1]

[1]ONERA - Université Paris Saclay, Department of Materials and Structures
29, avenue de la Division Leclerc, BP 72 - 92322 Châtillon Cedex - France
Email: martin.hirsekorn@onera.fr, Web Page: www.onera.fr

Keywords: woven composites, multiscale modeling, crack initiation, damage observation, digital image correlation

Abstract

Damage onset and evolution in a polymer matrix composite with woven reinforcement is observed at the micro- and mesoscale with the aid of digital image correlation (DIC) with mechanical regularization. At the microscale, damage is modeled using cohesive zone mdoels (CZM) to simulate the initial fiber-matrix debonding. An experimentally identified large strain viscoplastic model is used for the polymer matrix to simulate te evolution and stretching of matrix bands between the debondings and the subsequent coalescence into a transverse yarn crack. At the mesoscale, incremental fracture mechanics is used to predict the initiation and propagation of yarn cracks and yarn-yarn debondings, including coupling between cracks in the same yarn. The evolution of the crack and debonding density with increasing macroscopic strain is calculated and compared to experimental data obtained by automated detection of cracks and debondings from DIC residuals. The influence of these damages on the macroscopic properties of the composite obtained numerically is in good agreement with the experimental observations on macroscopic composite specimens.

1. Introduction

The prediction of strength and lifetime of composites by numerical models starting from the mechanical behavior of its constituents and the manufacturing process parameters remains an open challenge, which limits the competitiveness of composite materials in industrial applications due to the high design costs of composite structures. Frequently, composite materials are not optimally adapted to a specific structural application, because extensive testing campaigns are necessary - due to a lack of predicitve numerical models - to determine the optimum material choice. A complete bottom-up modeling approach is probably irrealistic, because of the difficulties of direct indentification of, e.g., the in-situ mechanical behavior of the polymer matrix or the properties of the fiber-matrix interfaces . However, multi-scale modeling strategies taking into account the damage mechanisms over the whole range of characteristic scales of a composite provide a large potential for at least predicting the trends of the mechanical properties when the constituents or the reinforcement architecture are modified.

In most composite materials, three characteristic scales can be identified [1]. The microscale, at which the constituent materials (fibers and matrix) are treated individually, the mesoscale, at which the architecture of the reinforcement is modeled and ensembles of a large number of fibers (e.g., plies or yarns) are treated as homogeneous material, and the macroscale, at which simulations of the structure take place and at which the entire composite material is treated as homogeneous material. The relevance of the different scales on damage evolution depends on the application. While mesoscale approaches are sufficient for most quasi-static load cases if mainly the influence of the reinforcement architecture is taken into account, the microscale becomes important if the influence of the constituent materials and their interfaces or the effects of fatigue loading are considered.

The two most common approaches to model damage onset and evolution at the mesoscale are based on continuum mechanics [1-3] or discrete damage models with direct insertion of the cracks in the Finite Element (FE) meshes of the mesoscale unit cells [4-6]. The main difficulty in continuum mechanics based approaches is to overcome mesh dependencies due to damage localization, which requires regularization methods [7-8] in order to avoid erroneous predictions of damage propagation directions [1,9]. Discrete damage models require *a priori* knowledge of the crack positions or high computational costs to determine them numerically [5-6].

At the microscale, damage starts with debonding of the fibers from the matrix, which implies that the onset location of the first damages is well known. Therefore, the most common approaches to model fiber-matrix debonding are cohesive zone models (CZM), which are inserted at the fiber-matrix interfaces [10-12]. Computationally more efficient are boundary element methods with linear elastic brittle interface models [13-14]. However, FE-based approaches provide a more convenient framework for modeling matrix plastification, which takes place between fiber-matrix debonding and the generation of a mesoscale crack [10-12].

Multi-scale modeling of damage in composites with complex reinforcement architectures, such as woven fabrics, require thus complex models with a large number of parameters. Therefore, experimental identification at the different scales plays a key role. In recent years, digital image correlation (DIC) was increasingly used to measure the strain fields on the surface of specimens both at the mesoscale [15-16] and the microscale [17-19]. This information about the full heterogeneous strain fields provides a powerful tool to validate the in-situ behavior of the constituents within a composite at different scales.

In this contribution, the damage observed at the micro- and mesoscale of a composite made of a 5-harness satin reinforcement of carbon fibers and the RTM6 epoxy resin and its visualization with the aid of DIC is presented. Based on these observations, numerical models are proposed to simulate damage onset and evolution at microscale (section 2) and at the mesoscale (section 3).

2. Damage at the microscopic scale

2.1. Experimental observations

The evolution of damage at the microscale is observed by means of tensile tests in-situ in a scanning electron microscope (SEM). The specimen surface was covered by a speckle pattern of aluminum particles following a technique similar to [18], in order to provide sufficient information to measure the full displacement fields by DIC both in the yarns and in resin rich regions, which otherwise present no contrast. The first damage observed is fiber-matrix debonding in the yarns oriented in transverse direction with respect to the loading direction (Fig. 1a). These initial debondings appear around many fibers located everywhere in the yarn. Only at a later loading stage, the debondings open further along a privileged path (Fig 1b). The matrix bands between the debonded interfaces undergo large plastic stretching before failure and subsequent coalescence into a transverse yarn crack.

A global approach of DIC together with a mechanical regularization [20] specially adapted to heterogeneous materials with high property contrast [19] is used to measure the displacement of the fibers and within the matrix. The regularization ensures a mechanically admissible displacement field even in regions where the speckle pattern provides insufficient information for a classical local DIC. The mechanical regularization does not take into account displacement discontinuities, which has the consequence that the correlation residual is particularly high at the fiber-matrix debondings. This effect can be used for damage detection (see section 3.1).

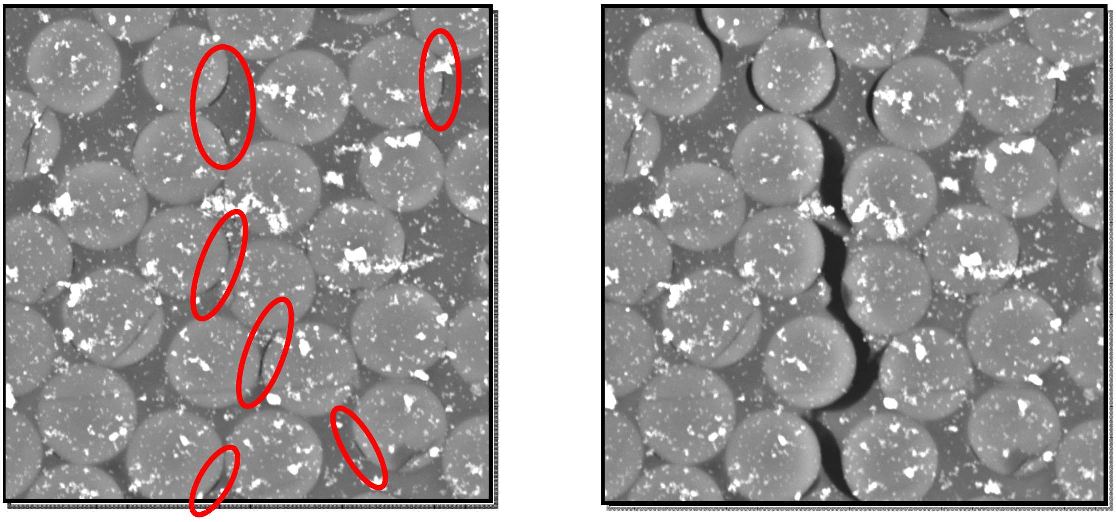

(a) (b)

Figure 1. SEM observations of the initiation of a transverse yarn crack: (a) fiber-matrix debonding and (b) crack coalescence with plastic stretching of matrix bands.

2.2. Mechanical behavior of the constituents

A large strain viscoplastic model based on [21] was identified using published experimental data [22] and testing results obtained at Onera (Fig. 2a). The kinematic hardening rules were adapted to reproduce the hysteresis and strain accumulation under compressive cyclic loading (Fig. 2b). This increase of plastic strain may contribute to damage evolution at the microscale under fatigue loading. Macroscopic matrix specimens undergo brittle failure at relatively low strains under tension, starting from surface flaws. However, at the microscale of composites, the size of the plastification zone around the fiber-matrix debondings is comparable to the fiber diameters. Therefore, at this scale, significant plastic strain is observed even under tension. A Raghava-type yield criterion is used to distinguish between yielding under tension and compression. The carbon fibers are modeled as transverse isotropic elastic material.

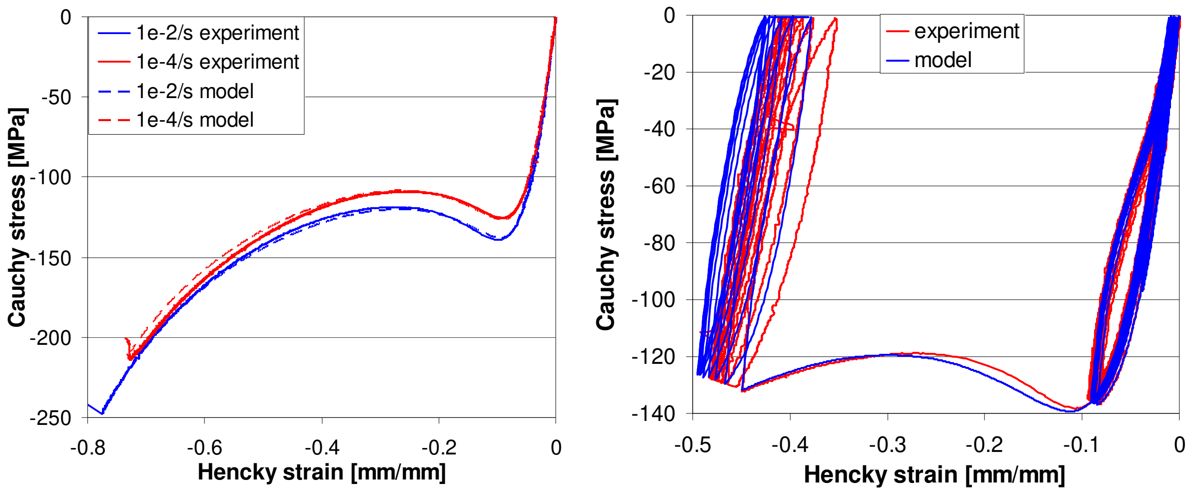

(a) (b)

Figure 2. Experimentally observed and modeled mechanical behavior of the RTM6 resin under monotonic (a) and cyclic compression (b).

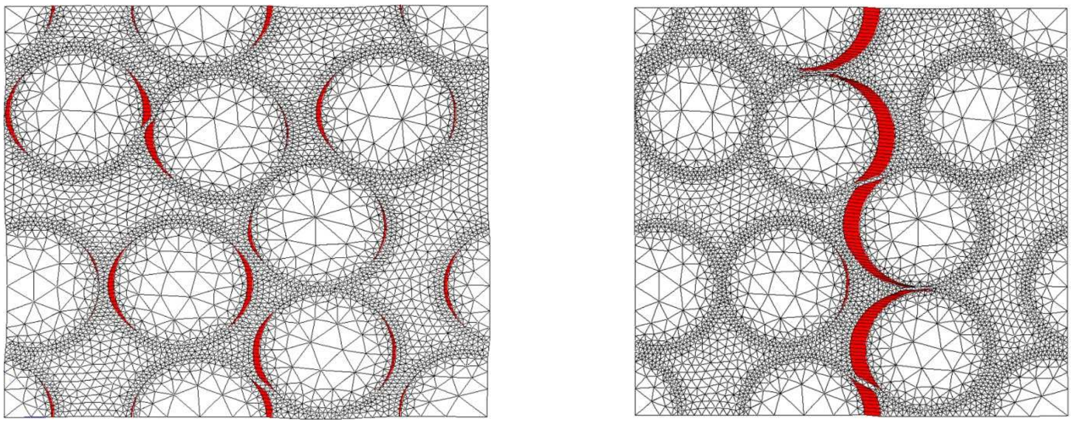

(a) (b)

Figure 3. Micro-scale modeling of a yarn crack initiation: (a) fiber-matrix debonding (displacements enlarged by a factor of 20 for visualization of the debondings) and (b) crack coalescence with plastic stretching of matrix bands.

2.3. Results

FE meshes of different microscale unit cells were generated with periodic random fiber distributions (Fig. 3) or fiber positions taken from SEM images. Fiber-matrix debonding is modeled using bilinear CZM with different strength values between 20 and 90MPa and a fracture energy in mode I of $2 J/m^2$ [14]. The interface strength has a direct impact on the maximum average stress reached in the unit cell, while the fracture energy only influences the stress decrease after the maximum. Likewise, for unit cells containing periodic random distributions of as few as 9 fibers, the fiber distribution only influences the stress decrease after the maximum. If the interface strength is significantly lower than the matrix yield peak (about 100MPa under tension), fiber-matrix debondings are generated at most of the fibers in the loading direction and at both sides of the fibers (Fig. 3a). After the generation of these debondings, the average stress of the unit cell decreases with increasing average strain.

At a slightly higher applied global strain, the debondings continue to open only along a privileged crack path, which depends on the fiber distribution (Fig. 3b). The interfaces far from this crack path close again, as the global load decreases. The matrix band between the debondings deform plastically up to very large strains limited by the hardening effect due to chain stretching (Fig. 2a). Failure of the matrix bands is modeled by removing the matrix elements from the integration once the maximum principal strain reaches a value of 0.6 (arbitrarily chosen to be located within the chain stretching zone and above the yield peak). During the matrix band stretching, the average stress over the unit cell is approximately constant at about 10MPa, which is significantly lower than the maximum stress. However, since the matrix bands are streched to very large deformations, the energy dissipated during this part of the crack coalescence makes a significant contribution to the total fracture energy of the unit cell.

3. Damage at the mesoscopic scale

3.1. Experimental observations

At the mesoscopic scale, before final failure of the composite specimen under tension, an increasing number of cracks is observed in the yarns transverse to the loading direction. These cracks are accompanied by yarn-yarn debondings around the crack tips. These debondings are difficult to see on the optical microscope images, but can be detected using DIC. The method presented in section 2.1 is applied to optical microscope images of the unloaded and the loaded specimens after having been

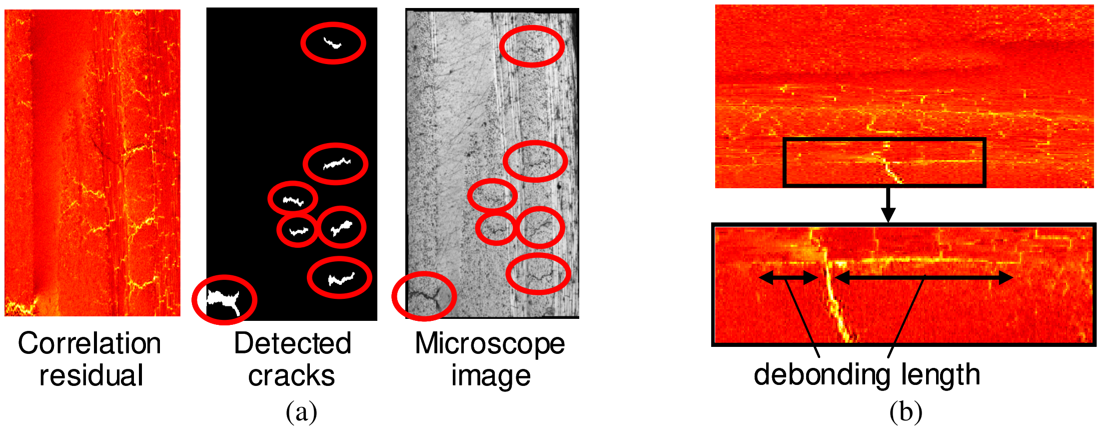

Figure 4. (a) Crack detection from the correlation residual and identification of the cracks on the microscope image. (b) Determination of the debonding length from the correlation residual.

exposed to different maximum loads, in order to generate different crack densities. At the mesoscale, it is not necessary to apply a speckle pattern, as the fibers within the yarns provide a sufficiently heterogeneous structure for the DIC to succeed, at least if mechanical regularization is used [6,20]. As can be seen in Fig. 4a, the correlation residual is particularly high at the yarn crack locations, because the displacement discontinuity around these cracks is not taken into account in the mechanical regularization. Therefore, the maps of the correlation residual can be used after some image treatment (see Fig. 4a) to automatically detect and count the transverse yarn cracks. Furthermore, it is shown in Fig. 4b, that the displacement discontinuity parallel to the yarn-yarn interfaces at the debonded zones also generates a high correlation residual. Therefore, the length of the debonded zones around the crack tips can be determined much more precisely from the correlation residual than from the microscope image shown in Fig. 4a, where the debondings can hardly be identified.

3.2. Modeling of yarn crack initiation

Crack initiation at weak stress singularities or non-singular stress states can be modeled using a coupled criterion composed of a strength and a toughness condition [23]. The strength condition is given by a stress-based criterion initially developed to predict the strength of uniaxial plies in laminates [24-25]. The toughness condition is based on the principles of Finite Fracture Mechanics (FFM) [26], which states that cracks of finite size may initiate instantaneously. According to the coupled criterion [23], the stress criterion must be fulfilled over the whole crack surface.

In the case of the studied woven composites, it was shown [5] that for transverse yarn cracking the toughness condition is fulfilled at higher global strains than the strength condition. Transverse yarn crack initiation is thus governed by FFM. However, even at global strains sufficiently high to allow transverse yarn cracking, the stress criterion is not fulfilled on the yarn-yarn interfaces. Therefore, following the theory of [23], there is no yarn-yarn debonding at crack initiation. Though, since the stress becomes singular at the crack tip, yarn-yarn debondings may initiate as soon as a transverse yarn cracks are present [5-6]. The initial debond length right after crack initiation is predicted using the same approach as for the yarn crack initiation [5].

3.3. Modeling of debonding and crack propagation

Once a yarn crack and a debonding around the crack tip have initiated, the stress state is strongly singular at the crack and debonding fronts. Classical fracture mechanics can thus be used to model the propagation of cracks and debondings [6]. For each crack/debonding configuration, the energy release rate for crack and debonding propagation is calculated by FE calculations on a mesoscale unit cell of

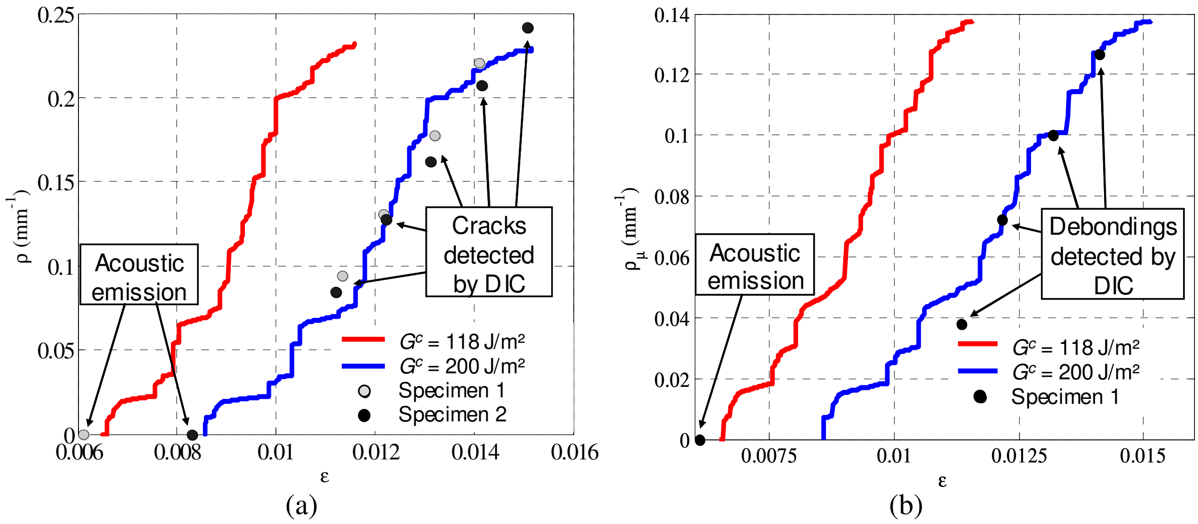

Figure 5. Simulated evolution of crack (a) and debonding density (b) for two different values of G^c in comparison with the crack and debonding densities detected by DIC.

the composite, taking into account the deformation of the yarns and the nesting between the fabric layers during the forming process [16,25]. It was shown that after the initiation of the yarn-yarn debonding, the energy release rate for crack propagation is always higher than for an increase of the debonding length [6]. Therefore, the mesoscale damage sequence is the following: transverse yarn cracks initiate at a finite length given by FFM, followed immediately by the onset of yarn-yarn debondings of finite lengths around the crack tips. Then the cracks propagate through the yarns parallel to the fibers at constant debonding lengths.

3.4. Results

The crack and debonding density evolution calculated using the described method is presented in Fig. 5 as a function of the global strain on the specimens, and compared to experimentally observed crack and debonding densities (section 3.1). In a first run, a fracture energy of 118J/m^2 [27] was used for both transverse yarn cracking and yarn-yarn debonding. Good agreement with the strain at the first crack initiation was observed [5]. However, repeating the study on further specimens showed a large dispersion of the strains at first crack initiation, while the evolution of the crack density (total crack area per volume), which is an average quantity over a large number of cracks, is much less dispersed. A fracture energy of 200J/m^2 produced a good agreement of the numerical simulations with the experimentally observed crack density evolution. Furthermore, the strain at first crack initiation also lies within the range of the experimental observations. Using the same fracture energy for yarn-yarn debonding in the numerical simulations gave an evolution of the debonding density in good agreeement with the debonding lengths observed by DIC (section 3.1).

4. Conclusions

DIC is a powerful tool to observe the full strain fields on the surface of specimens. In particular, in the case of heterogeneous materials, strain can be measured within the different constituents, which allows validating mechanical models for the constituents in-situ in the composite. Mechanical regularization ensures continuous and mechanically admissible displacement fields and provides information on the local displacement even in zones where the contrast at the specimen surface is low. Displacement discontinuities caused by damage are incompatible with the mechanical regularization. The resulting high correlation residual at the locations of damage can be used to detect cracks automatically and to measure debonding lengths, which are difficult to observe on optical microscope images.

The proposed modeling strategies reproduce well the experimentally observed damage sequences at the micro- and the mesoscale. At the microscale, matrix plasticity has not only to be taken into account to correctly model the coalescence of the fiber-matrix debondings into a transverse yarn crack, but cumulated plastic strain during cyclic loading may also contribute to the evolution of fatigue damage at the microscale. At the mesoscale, the zones of plastification are much smaller than the characteristic size of the different entities. Therefore, the yarns behave like a brittle material, and fracture mechanics based approaches can be used to predict crack initiation and propagation. This is confirmed by experimental observations that show discrete yarn cracks without any visible damage at the mesoscale in their surroundings. The proposed method based on a coupled strength and toughness criterion shows that yarn crack initiate without yarn-yarn debondings. However, these debondings initiate immediately after yarn cracking. Propagation of the yarn cracks at constant debonding length is energetically more faborable than an increase of the debonding length. The numerically obtained crack and debonding densities are in good agreement with experimental observations if the same fracture energy is used for yarn cracking and yarn-yarn debonding.

Acknowledgments

Some of the work mentioned in section 2 (experimental testing of the RTM6 resin, microscale damage modeling) was carried out in collaboration with SAFRAN Composites (B. Tranquart) and the LMT Cachan (E. Baranger). For the DIC with mechanical regularization, the software Correli RT3 [20] developed at LMT Cachan was used. The help of F. Hild and E. Baranger is gratefully acknowledged.

References

[1] S.V. Lomov, D.S. Ivanov, I. Verpoest, M. Zako, T. Kurashiki, H. Nakai, and S. Hirosawa. Meso-FE modelling of textile composit es: Road map, data flow and algorithms. *Composites Science and Technology*, 67:1870-1891, 2007.
[2] S. Daggumati, W. Van Paepegem, J. Degrieck, J. Xu, S.V. Lomov, and I. Verpoest. Local damage in a 5-harness satin weave composite under static tension: Part II – Meso-FE modelling. *Composites Science and Technology*, 70:1934-1941, 2010.
[3] P. Melro, P. Camanho, F.M. Andrade Pires, and S.T. Pinho. Numerical simulation of the non-linear deformation of 5-harness satin weaves. *Computational Materials Science*, 61:116-126, 2012.
[4] E. Obert, F. Daghia, P. Ladevèze, and L. Ballere. Micro and meso modeling of woven composites: transverse cracking kinetics and homogenization. *Composite Structures*, 117:212-221, 2014.
[5] A. Doitrand, C. Fagiano, N. Carrère, V. Chiaruttini, and M. Hirsekorn. Damage onset modeling in woven composites based on a coupled stress and energy criterion. *Engineering Fracture Mechanics*, 169:189-200, 2017.
[6] A. Doitrand, C. Fagiano, F. Hild, V. Chiaruttini, A. Mavel, and M. Hirsekorn. Mesoscale analysis of damage growth in woven composites. *Composites: Part A*, 96:77-88, 2017.
[7] O. Allix, P. Feissel, and P. Thevenet. A delay damage mesomodel of laminates under dynamic loading: basic aspects and identification issues. *Computers & Structures*, 81:1177-1191, 2003.
[8] P. Maimí, P.P. Camanho, J.A. Mayugo, and C.G. Davila. A continuum damage model for composite laminates: Part II – Computational implementation and validation. *Mechanics of Materials*, 39:909-919, 2007.
[9] L. Gorbatikh, D. Ivanov, S.V. Lomov, and I. Verpoest. On modelling of damage evolution in textile composites on meso-level via property degradation approach. *Composites: Part A*, 38:2433-2442, 2007.
[10] E. Totry, C. González, and J. LLorca. Influence of the loading path on the strength of fiber-reinforced composites subjected to transverse compression and shear. *International Journal of Solids and Structures*, 45:1663-1675, 2008.

[11] L.P. Canal, C. González, J. Segurado, and J. LLorca. Intraply fracture of fiber-reinforced composites: Microscopic mechanisms and modeling. *Composites Science and Technology*, 72:1223-1232, 2012.
[12] F. Naya, C. González, C.S. Lopes, S. Van der Veen, and F. Pons. Computational micromechanics of the transverse and shear behavior of unidirectional fiber reinforced polymers including environmental effects. *Composites: Part A*, 92:146-157, 2017.
[13] V. Mantič and I.G. García. Crack onset and growth at the fibre–matrix interface under a remote biaxial transverse load. Application of a coupled stress and energy criterion. *International Journal of Solids and Structures*, 49:2273-2290, 2012.
[14] L. Távara and V. Mantič. Crack paths formed by multiple debonds in LFRP composites. *Mechanics Research Communications*, 84:148-154, 2017.
[15] S. Daggumati, E. Voet, W. Van Paepegem, J. Degrieck, J. Xu, S.V. Lomov, and I. Verpoest. Local strain in a 5-harness satin weave composite under static tension: Part I – Experimental analysis. *Composites Science and Technology*, 71:1171-1179, 2011.
[16] A. Doitrand, C. Fagiano, F.-H. Leroy, A. Mavel, and M. Hirsekorn. On the influence of fabric layer shifts on the strain distributions in a multi-layer woven composite. *Composite Structures*, 145:15-25, 2016.
[17] L.P. Canal, C. González, J.M. Molina-Aldareguía, J. Segurado, and J. LLorca. Application of digital image correlation at the microscale in fiber-reinforced composites. *Composites: Part A*, 43:1630-1638, 2012.
[18] M. Mehdikhani, M. Aravand, B. Sabuncuoglu, M.G. Callens, S.V. Lomov, and L. Gorbatikh. Full-field strain measurements at the micro-scale in fiber-reinforced composites using digital image correlation. *Composite Structures*, 140:192-201, 2016.
[19] R. Naylor, F. Hild, C. Fagiano, M. Hirsekorn, Y. Renollet, B. Tranquart, and E. Baranger. Full-field displacement measurement by mechanically regularised global Digital Image Correlation for heterogeneous materials. *In preparation*.
[20] Z. Tomičević, F. Hild, and S. Roux. Mechanics-aided digital image correlation. *The Journal of Strain Analysis for Engineering Design*, 48:330-343, 2013.
[21] N.M. Ames, V. Srivastava, S.A. Chester, and L. Anand. A thermo-mechanically coupled theory for large deformations of amorphous polymers. Part II: Applications. *International Journal of Plasticity*, 25:1495-1539, 2009.
[22] X.P. Morelle, F. Lani, M.A. Melchior, S. André, C. Bailly, and T. Pardoen. The elasto-viscoplasticity and fracture behaviour of the RTM6 structural epoxy and impact on the response of woven composites. *Proceedings of the 15th European Conference on Composite Materials (ECCM15), Venice, Italy*, June 24-28 2012.
[23] D. Leguillon. Strength or toughness? A criterion for crack onset at a notch. *European Journal of Mechanics A/Solids*, 21:61-72, 2002.
[24] F. Laurin, N. Carrère, and J.F. Maire. A multiscale progressive failure approach for composite laminates based on thermodynamical viscoelastic and damage models. Composites Part A, 38:198-209, 2007.
[25] A . Doitrand, C. Fagiano, V. Chiaruttini, F.H. Leroy, A. Mavel, and M. Hirsekorn. Experime ntal characteriz ation and numerica l modeling of damage at the mesosc opic scale of woven polymer matrix compo sites under quasi-static tensile loading. *Composites Science and Technology*, 119:1-11, 2015.
[26] P. Weißgraeber, D. Leguillon, W. Becker. A review of Finite Fracture Mechanics: crack initiation at singular and non-singular stress raisers. *Archives of Applied Mechanics*, 86:375-401, 2016.
[27] M. Benzeggagh and M. Kenane. Measurement of mixed-mode delamination fracture toughness of unidirectional glass/epoxy composites with mixedmode bending apparatus. *Composites Science and Technology*, 56:439-49, 1996.